

ICGSEE-2013[14th – 16th March 2013]
International Conference on Global Scenario in Environment and Energy

A CFD Analysis Of A Solar Air Heater Having Triangular Rib Roughness On The Absorber Plate

Anil Singh Yadav*, J.L.Bhagoria

**Mechanical Engineering Department, Maulana Azad National Institute of Technology,
Bhopal, MP 462051, India.**

***Corres.author: anilsinghyadav@gmail.com
Tel.: +919229220126.**

Abstract: This paper presents the study of heat transfer in a rectangular duct of a solar air heater having triangular rib roughness on the absorber plate by using Computational Fluid Dynamics (CFD). The effect of Reynolds number on Nusselt number was investigated. The computations based on the finite volume method with the SIMPLE algorithm have been conducted for the air flow in terms of Reynolds numbers ranging from 3000-18000. A commercial finite volume package ANSYS FLUENT 12.1 is used to analyze and visualize the nature of the flow across the duct of a solar air heater. CFD simulation results were found to be in good agreement with experimental results and with the standard theoretical approaches. It has been found that the Nusselt number increases with increase in Reynolds number.

Key words: Solar Air Heater, Heat transfer, CFD.

1. Introduction

Solar air heater is one of the basic equipment through which solar energy is converted into thermal energy. Solar collectors in the system for the utilization of solar thermal energy are widely used in various equipment. Solar collectors (air heaters), because of their simple in design, are cheap and most widely used collection devices of solar energy. The main application of solar air heaters are space heating, seasoning of timber, curing of industrial products and these can also be effectively used for curing/drying of concrete/clay building components^{1,2}.

There seems to be lack of computational works on prediction of heat transfer and fluid flow using CFD in solar air heater. Number of experimental studies³⁻⁵ have been carried out to evaluate performance of solar air heater but very few attempts of CFD investigation have been made so far due to complexity of flow pattern and computational limitations. With the development of computer, hardware and numerical methodology, advanced mathematical models are being used to carry out critical investigations on solar air heaters. The advantages of computational simulations are that they can produce extremely large volumes of results at virtually no added expense and it is very cheap to perform parametric studies to optimize equipment performance. The second reason for such work on computational simulation is that some parameters are difficult to test, and experimental

study is expensive as well as time consuming. The results obtained with the CFD are of acceptable quality. Chaube et al⁶. is carried out a 2-D computational analysis to assess the comparative performance of the absorber plate of a solar air heater with different roughness elements using commercial software package FLUENT 6.1. The assessment was based on heat transfer enhancement with minimum pressure penalty. Ten different rib shapes viz. Rectangular, Square, Chamfered, Triangular, Semicircle etc., were investigated at the Reynolds number range from about 3000–20000, in which solar air heaters normally operate. Kumar and Saini⁷ carried out CFD based analysis to fluid flow and heat transfer characteristics of a solar air heaters having roughened duct provided with artificial roughness in arc shaped geometry. The heat transfer and flow analysis of the chosen roughness element were carried out using 3-D models. Authors reported that Nusselt number has been found to increase with increase in Reynolds number where friction factor decreases with increase in Reynolds number for all combinations of relative roughness height (e/D) and relative arc angle ($\theta/90$). Karmare and Tikekar⁸ performed a CFD simulation of fluid flow and heat transfer in a solar air heater duct with metal grit ribs as roughness elements employed on one broad wall of a solar air heater. The circular, triangular and square shape rib grits with the angle of attack of 54°, 56°, 58°, 60° and 62° were tested for the same Reynolds number. Authors reported that the CFD results give the good agreements with experimental results. Hence, CFD techniques can be used for analyzing and optimizing complex type of roughness surface. Soi et al⁹. presented a CFD based investigation of heat transfer and friction characteristics of artificially roughened duct of a solar air heater. K-shaped (combination of transverse and V-up) roughness geometry was used as an artificial roughness. Authors observed, for a given type of artificial roughness, Nusselt number increases with an increase in Reynolds number for smooth as well as roughened plate. Sharma et al¹⁰. designed a solar air heater duct in order to carry out CFD based investigation. CFD based performance analysis of solar air heater duct provided with artificial roughness in the form of square type protrusion shape geometry was reported. 2-D computational domain and grid were selected. Non-uniform meshing was generated over the duct. Sharma and Thakur¹¹ conducted a CFD study to investigate the heat transfer and friction loss characteristics in a solar air heater having attachments of V-shaped ribs roughness at 60° relative to flow direction pointing downstream on underside of the absorber plate. Authors observed, Nusselt number increases with increase in Reynolds number where friction factor decreases with increase in Reynolds number for all combinations of relative roughness height (e/D) and relative roughness pitch.

In the present work a computational investigation of turbulent forced convection in a two-dimensional duct of a solar air heater having triangular rib roughness on the absorber plate is conducted. The upper wall is subjected to a uniform heat flux condition while the lower wall and two other side walls, except inlet and outlet are insulated.

2. Thermal Performance Of Solar Air Heater

Thermal performance concerns with heat transfer process within the collector. A conventional solar air heater shown in Fig. 1 is considered for brief analysis of thermal performance. Design and construction detail of such type of a conventional system are described by Garg and Prakash¹.

Thermal performance of solar air heater can be computed with the help of Hottel–Whillier–Bliss equation reported by Duffie and Beckman².

$$Q_u = A_c F_R [I(\tau\alpha)_e - U_L(T_i - T_a)] \quad (1)$$

or

$$q_u = \frac{Q_u}{A_c} = F_R [I(\tau\alpha)_e - U_L(T_i - T_a)] \quad (2)$$

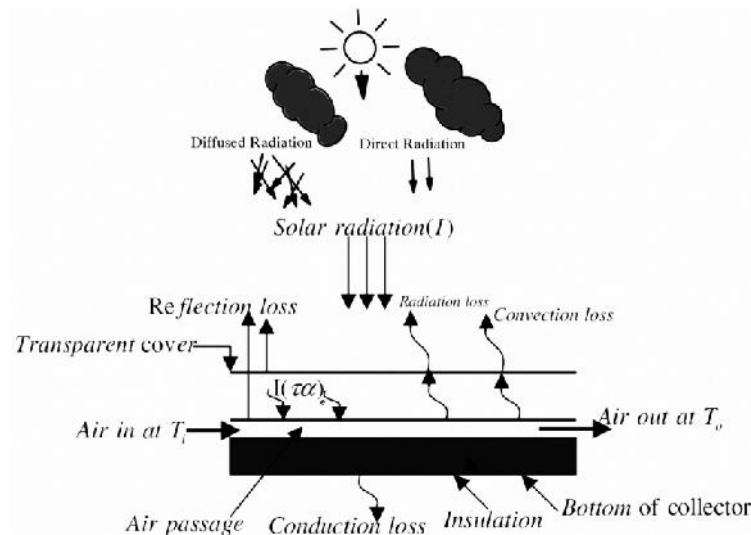


Figure 1 Solar air heater.

The rate of valuable energy gain by flowing air in the course of duct of a solar air heater can be intended as follows equation:

$$Q_u = \dot{m} c_p (T_o - T_i) = h A_c (T_{pm} - T_{am}) \quad (3)$$

The value of heat transfer coefficient (h) can be increased by various active and passive augmentation techniques. It can be represented in non-dimensional form of Nusselt number (Nu).

$$Nu = hl/k \quad (4)$$

Further, thermal efficiency of a solar air heater can be expressed by the following equation;

$$\eta_{th} = \frac{Q_u}{I} = F_R [(\tau\alpha)_e - U_L(T_i - T_a)/I] \quad (5)$$

3. Computational Fluid Dynamics Approach

Computational fluid dynamics or CFD is the analysis of systems involving fluid flow, heat transfer and associated phenomena such as chemical reactions by means of computer-based simulation. The technique is very powerful and spans a wide range of industrial and non-industrial application areas.

Dynamics of fluids are governed by coupled non-linear partial differential equations, which are derived from the basic physical laws of conservation of mass, momentum, and energy. Analytical solutions of such equations are possible only for very simple flow domains with certain assumptions made about the properties of the fluids involved. For conventional design of equipment, devices, and structures used for controlling fluid flow patterns, designers have to rely upon empirical formulae, rules of thumb, and experimentation. However, there are many inherent problems with these conventional design processes. Empirical formulae and rules of thumb are extremely specific to the problem at hand and are not globally usable because of the non-linearity of the governing equations. For example, a rule of thumb for designing an aircraft wing may not be applicable for designing a wing mounted on a racing car, as the upstream flow conditions are completely different for the two configurations.

The above reasons make experimentation the leading conventional design technique. However, there are many limitations of experimentation techniques as well:

- ⌘ Measurement of flow variables may cause these variables themselves to change, might not be possible at all (in very small or unreachable spaces), and may be expensive.
- ⌘ Experimentation may take a long time to set up, sometimes lasts for a very short time, and may be very expensive, as in the case of supersonic wind-tunnel runs.
- ⌘ Experimental data has limited detail.

All these limitations are overcome by CFD, since it is a numerical simulation technique which does not require a prototype to be built, is not thwarted by measurement capabilities, and can provide extremely detailed data as and when required. Using CFD, we can build a computational model that represents a system or device that we want to study. Then we apply the fluid flow physics to this virtual prototype, and the software provides a prediction of the fluid flow pattern and other physical phenomena. CFD analysis not only complements testing and experimentation, but leads to a substantial saving of time as a large number of options can be tested much before the prototyping stage.

CFD codes are structured around the numerical algorithms that can tackle fluid flow problems. In order to provide easy access to their solving power all commercial CFD packages include sophisticated user interfaces to input problem parameters and to examine the results.

4. CFD Analysis

4.1. Computational Domain

The 2-D computational domain used for CFD analysis having the height (H) of 20 mm and width (W) 100 mm and total length of 461 mm as shown in Fig 2.

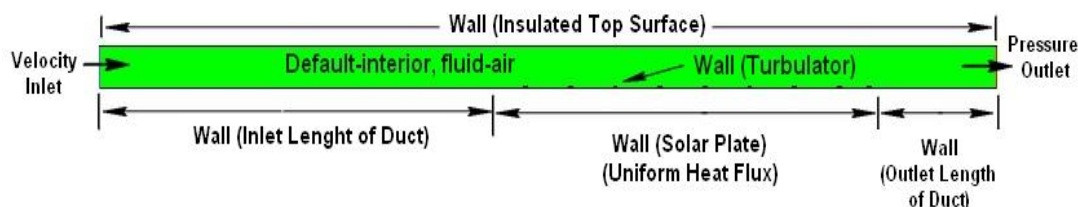


Figure 2 Two dimensional computational domain.

Complete duct geometry is divided into three sections, namely, entrance section, test section and exit section. A short entrance length is chosen because for a roughened duct, the thermally fully developed flow is established in a short length 2–3 times hydraulic diameter. The exit section is used after the test section in order to reduce the end effect in the test section. Roughness geometry in the triangular shape on the roughened absorber plate has been shown in Fig. 3.

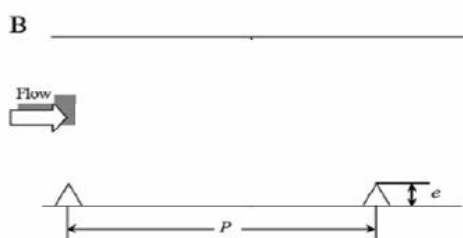


Figure 3 Triangular shaped rib roughness.

Operating and geometrical parameters of the artificially roughened solar air heater duct for computational analysis are shown in table 1.

Table 1: Parameters of the artificially roughened solar air heater duct for computational analysis

Relative roughness pitch, p/e	10, 12, 14
Heat Flux, I	1000 W/m^2
Reynolds number range	3000 - 18000
Duct depth, H	20 mm
Duct width, W	100 mm
Hydraulic diameter, D_h	33.33 mm
Relative roughness Height, e / D_h	0.03
Rib height, e	1 mm
Plate length, L	121 mm

In the present study, FLUENT Version 12.1 is used for analysis.

The following assumptions are imposed for the computational analysis.

- (1) The flow is steady, fully developed, turbulent and two dimensional.
- (2) The thermal conductivity of the duct wall, absorber plate and roughness material are independent of temperature.
- (3) The duct wall, absorber plate and roughness material are homogeneous and isotropic.
- (4) The working fluid, air is assumed to be incompressible for the operating range of solar air heaters since variation in density is very less.
- (5) No-slip boundary condition is assigned to the walls in contact with the fluid in the model.
- (6) Negligible radiation heat transfer and other heat losses.

4.2. Mesh Generation

After defining the computational domain, uniform meshing is done by rectangular elements. In creating this mesh, it is desirable to have more cells near the plate because we want to resolve the turbulent boundary layer, which is very thin compared to the height of the flow field. Fig. 4 shows the non-uniform quadrilateral meshing.

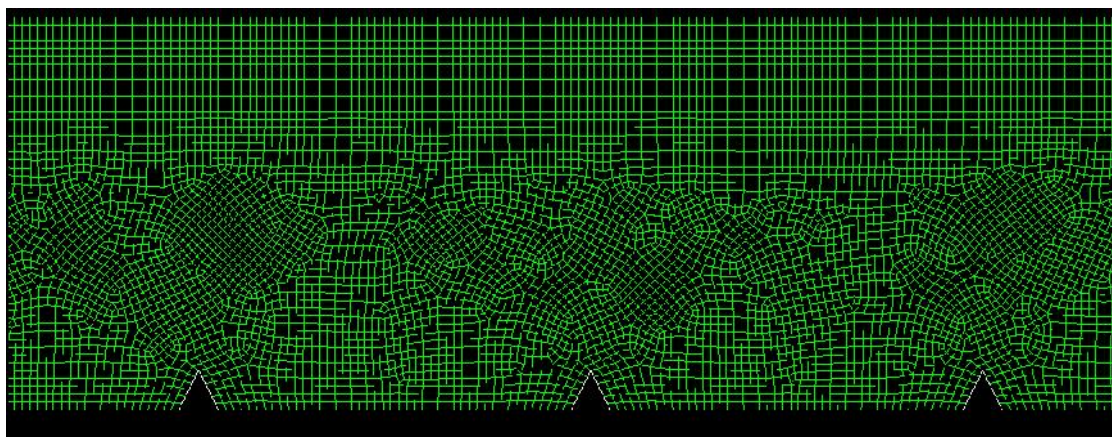


Figure 4A non-uniform quadrilateral meshing.

4.3. Boundary condition

Table 2 shows the detail of boundary conditions. The left edge was specified as the duct inlet and right edge as the duct outlet. Top edge was specified as top surface and bottom edges were inlet length, outlet length and solar plate. All internal edges of rectangle 2d duct were defined as turbulator wall.

Table 2 :Detail of boundary conditions

Edge Position	Name	Type
Left	Duct Inlet	VELOCITY_INLET
Right	Duct Outlet	PRESSURE_OUTLET
Top	Top Surface	WALL
Bottom edge-1	Inlet Length	WALL
Bottom edge-2	Solar Plate	WALL
Bottom edge-3	Outlet Length	WALL
Internal Edges of rectangle	Turbulator	WALL

4.4. Solver

FLUENT Version 12.1 is used as a solver with RNG k-epsilon turbulence model. The modeled turbulence kinetic energy, k , and its rate of dissipation, ϵ , are obtained from the following transport equations for Renormalization-group (RNG) k- ϵ model.

$$\frac{\partial}{\partial x_i} (\rho k u_i) = \frac{\partial}{\partial x_j} \left(\alpha_k \mu_{eff} \frac{\partial k}{\partial x_j} \right) + G_k - \rho \epsilon \quad (6)$$

and

$$\frac{\partial}{\partial x_i} (\rho \epsilon u_i) = \frac{\partial}{\partial x_j} \left(\alpha_\epsilon \mu_{eff} \frac{\partial \epsilon}{\partial x_j} \right) + C_{1\epsilon} \frac{\epsilon}{k} (G_k) - C_{2\epsilon} \rho \frac{\epsilon^2}{k} - R_\epsilon \quad (7)$$

5. Results And Discussion

In the present simulation governing equations of continuity, momentum and energy are solved by the finite volume method in the steady-state regime. The numerical method used in this study is a segregated solution algorithm with a finite volume-based technique. The governing equations are solved using the commercial CFD code, ANSYS Fluent 12.1. A second-order upwind scheme is chosen for energy and momentum equations. The SIMPLE algorithm (semi-implicit method for pressure linked equations) is chosen as scheme to couple pressure and velocity. The convergence criteria of 10^{-3} for the residuals of the continuity equation, 10^{-6} for the residuals of the velocity components and 10^{-6} for the residuals of the energy are assumed. A uniform air velocity is introduced at the inlet while a pressure outlet condition is applied at the outlet. Adiabatic boundary condition has been implemented over the bottom duct wall while constant heat flux condition is applied to the upper duct wall of test section. Fig. 5 shows the temperature Contour for the triangular shape of ribs inserted in a solar air heater duct. The patterns of temperature contour at regions behind and ahead of the rib illustrate the overall temperature field and the degree of heat transfer. CFD predicts temperature contour pattern better at the regions ahead of the rib.

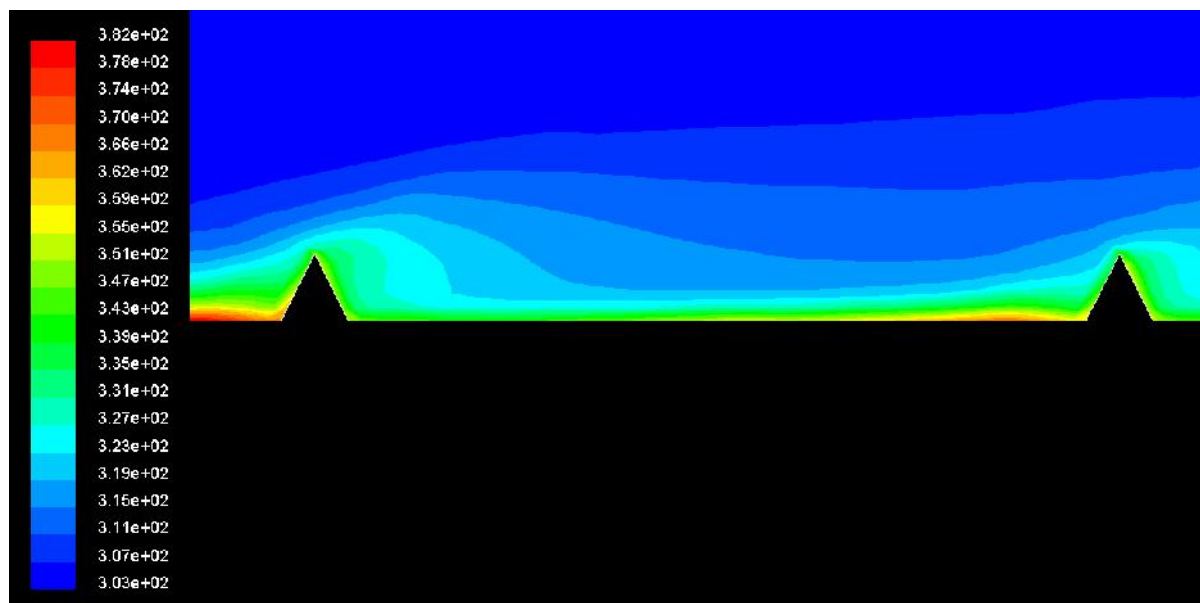


Figure 5 Temperature Contour

Fig. 6 shows the contour of stream function for the triangular shape of ribs inserted in a solar air heater duct. An observation of stream function contours reveals that vortex formation at top of the rib surface provides rolling action to the flow and hence reduces the friction.

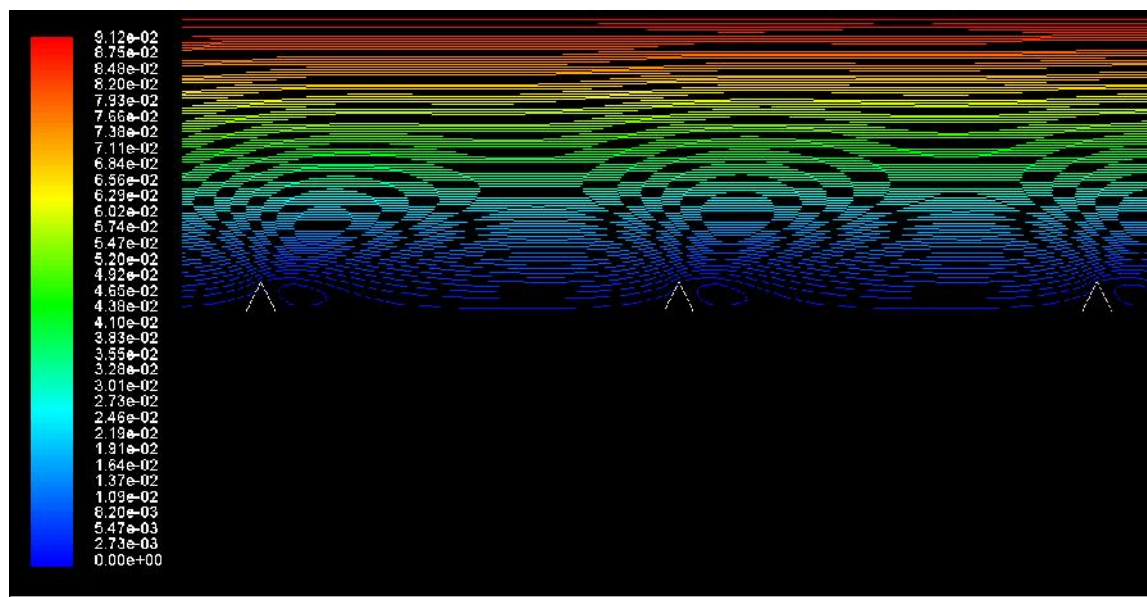


Figure 6 contour of stream function

CFD analysis predicts performance of triangular ribs at different p/e which is demonstrated through the Fig.7. It can be seen that there is a substantial enhancement caused by providing artificial roughness in the form of triangular rib roughness. The average Nusselt number is observed to increase with increase in Reynolds number due to the increase in turbulent intensity caused by increase in turbulent kinetic energy and turbulent dissipation rate. The heat transfer phenomenon can be observed and described by the contour of stream function. The enhancement in Nusselt number compared to that of the smooth surface achieved varies from 1.4 to 2.7 times. It can be seen from fig. 7 that the enhancement in heat transfer of the roughened duct with respect to the smooth duct also increases with an increase in Reynolds number. It can also be seen that Nusselt number values decrease with the increase in relative roughness pitch (P/e) for fixed value of relative roughness height, e/D . This is due to the fact that with the increase in relative roughness pitch, number of reattachment points over the absorber plate reduces.

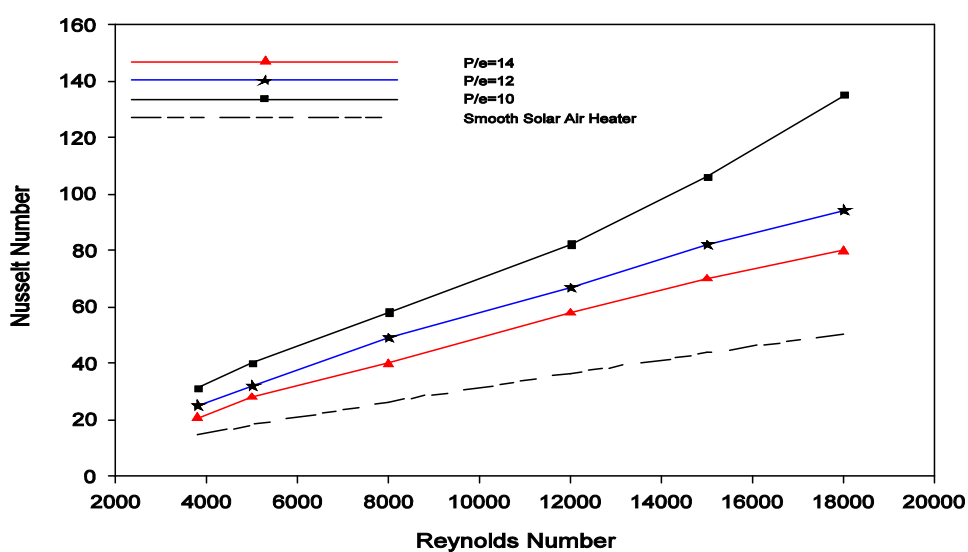


Figure 7: Nusselt number Vs Reynolds number

6. Conclusion

In this present investigation, a numerical prediction has been conducted to study heat transfer and flow friction behaviors of a rectangular duct of a solar air heater having triangular rib roughness on the absorber plate. The main conclusions are:

1. There is no doubt that a major focus of CFD analysis of solar air heater is to enhance the design process that deals with the heat transfer and fluid flow.
2. In recent years CFD has been applied in the design of solar air heater. The quality of the solutions obtained from CFD simulations are largely within the acceptable range proving that CFD is an effective tool for predicting the behavior and performance of a solar air heater.
3. Nusselt number increases with the increase of Reynolds number.
4. Solar air heater with triangular rib roughness gives 1.4 to 2.7 times enhancement in Nusselt number as compared to smooth duct.
5. The maximum value of Nusselt number has been found corresponding to relative roughness pitch of 10.

References

1. Garg H. P. and Prakash J., Solar Energy Fundamentals and Applications, 1st ed., Tata McGraw-Hill, New Delhi, 2000.
2. Duffie J. A. and Beckman W. A., Solar Engineering of Thermal Processes. 2nd ed., Wiley, New York, 1980.
3. Hans V. S., Saini R. P. and Saini J. S., Performance of artificially roughened solar air heaters- A review, Renewable and Sustainable Energy Reviews, 2009, 13, 1854–1869.
4. Bhushan B., Singh R., A review on methodology of artificial roughness used in duct of solar air heaters, Energy, 2010, 35, 202–212.
5. Patil A. K., Saini J. S. and Kumar K., A Comprehensive Review on Roughness Geometries and Investigation Techniques Used in Artificially Roughened Solar Air Heaters, International Journal of Renewable Energy Research, 2012, 2(1), 1-15.
6. Chaube A., Sahoo P. K. and Solanki S. C., Effect of Roughness Shape on Heat Transfer and Flow Friction Characteristics of Solar Air Heater with Roughened Absorber Plate, WIT Transactions on Engineering Sciences, 2006, 53, 43-51.
7. Kumar S. and Saini, R. P., CFD based Performance Analysis of a Solar Air Heater Duct Provided with Artificial Roughness, Renewable Energy, 2009, 34 (5), 1285-1291.
8. Karmare S. V. and Tikekar A. N., Analysis of Fluid Flow and Heat Transfer in a Rib Grit Roughened Surface Solar Air Heater using CFD, Solar Energy, 2010, 84 (3), 409-417.
9. Soi A. Singh, R. and Bhushan B., Effect of Roughness Element Pitch on Heat Transfer and Friction Characteristics of Artificially Roughened Solar Air Heater Duct, International Journal of Advanced Engineering Technology, 2010, 1(3), 339-346.
10. Sharma S., Singh, R. and Bhushan B., CFD based Investigation on Effect of Roughness Element Pitch on Performance of Artificially Roughened Duct used in Solar Air Heaters, International Journal of Advanced Engineering Technology, 2011, 2(1), 234-241.
11. Sharma A. K. and Thakur N. S., CFD based Fluid Flow and Heat Transfer Analysis of a V-Shaped Roughened Surface Solar Air Heater. International Journal of Engineering Science and Technology, 2012, 4(5), 2115-2121.
